Wess-Zumino Current and the Structure of the Decay $\tau^- \to K^-\pi^-K^+\nu_\tau$

T. E. Coan,[1] Y. S. Gao,[1] F. Liu,[1] R. Stroynowski,[1] M. Artuso,[2] C. Boulahouache,[2] S. Blusk,[2] J. Butt,[2] E. Dambasuren,[2] O. Dorjkhaidav,[2] J. Haynes,[2] N. Menaa,[2] R. Mountain,[2] H. Muramatsu,[2] R. Nandakumar,[2] R. Redjimi,[2] R. Sia,[2] T. Skwarnicki,[2] S. Stone,[2] J. C. Wang,[2] Kevin Zhang,[2] A. H. Mahmood,[3] S. E. Csorna,[4] G. Bonvicini,[5] D. Cinabro,[5] M. Dubrovin,[5] A. Bornheim,[6] E. Lipeles,[6] S. P. Pappas,[6] A. Shapiro,[6] A. J. Weinstein,[6] R. A. Briere,[7] G. P. Chen,[7] T. Ferguson,[7] G. Tatishvili,[7] H. Vogel,[7] M. E. Watkins,[7] N. E. Adam,[8] J. P. Alexander,[8] K. Berkelman,[8] V. Boisvert,[8] D. G. Cassel,[8] J. E. Duboscq,[8] K. M. Ecklund,[8] R. Ehrlich,[8] R. S. Galik,[8] L. Gibbons,[8] B. Gittelman,[8] S. W. Gray,[8] D. L. Hartill,[8] B. K. Heltsley,[8] L. Hsu,[8] C. D. Jones,[8] J. Kandaswamy,[8] D. L. Kreinick,[8] V. E. Kuznetsov,[8] A. Magerkurth,[8] H. Mahlke-Krüger,[8] T. O. Meyer,[8] J. R. Patterson,[8] T. K. Pedlar,[8] D. Peterson,[8] J. Pivarski,[8] D. Riley,[8] A. J. Sadoff,[8] H. Schwarthoff,[8] M. R. Shepherd,[8] W. M. Sun,[8] J. G. Thayer,[8] D. Urner,[8] T. Wilksen,[8] M. Weinberger,[8] S. B. Athar,[9] P. Avery,[9] L. Breva-Newell,[9] V. Potlia,[9] H. Stoeck,[9] J. Yelton,[9] B. I. Eisenstein,[10] G. D. Gollin,[10] I. Karliner,[10] N. Lowrey,[10] P. Naik,[10] C. Sedlack,[10] M. Selen,[10] J. J. Thaler,[10] J. Williams,[10] K. W. Edwards,[11] D. Besson,[12] K. Y. Gao,[13] D. T. Gong,[13] Y. Kubota,[13] S. Z. Li,[13] R. Poling,[13] A. W. Scott,[13] A. Smith,[13] C. J. Stepaniak,[13] J. Urheim,[13] Z. Metreveli,[14] K. K. Seth,[14] A. Tomaradze,[14] P. Zweber,[14] K. Arms,[15] E. Eckhart,[15] K. K. Gan,[15] C. Gwon,[15] H. Severini,[16] P. Skubic,[16] D. M. Asner,[17] S. A. Dytman,[17] S. Mehrabyan,[17] J. A. Mueller,[17] S. Nam,[17] V. Savinov,[17] G. S. Huang,[18] D. H. Miller,[18] V. Pavlunin,[18] B. Sanghi,[18] E. I. Shibata,[18] I. P. J. Shipsey,[18] G. S. Adams,[19] M. Chasse,[19] J. P. Cummings,[19] I. Danko,[19] J. Napolitano,[19] D. Cronin-Hennessy,[20] C. S. Park,[20] W. Park,[20] J. B. Thayer,[20] and E. H. Thorndike[20]

[1]*Southern Methodist University, Dallas, Texas 75275, USA*
[2]*Syracuse University, Syracuse, New York 13244, USA*
[3]*University of Texas–Pan American, Edinburg, Texas 78539, USA*
[4]*Vanderbilt University, Nashville, Tennessee 37235, USA*
[5]*Wayne State University, Detroit, Michigan 48202, USA*
[6]*California Institute of Technology, Pasadena, California 91125, USA*
[7]*Carnegie Mellon University, Pittsburgh, Pennsylvania 15213, USA*
[8]*Cornell University, Ithaca, New York 14853, USA*
[9]*University of Florida, Gainesville, Florida 32611, USA*
[10]*University of Illinois, Urbana-Champaign, Illinois 61801, USA*
[11]*Carleton University, Ottawa, Ontario, Canada K1S 5B6 and the Institute of Particle Physics, Canada*
[12]*University of Kansas, Lawrence, Kansas 66045, USA*
[13]*University of Minnesota, Minneapolis, Minnesota 55455, USA*
[14]*Northwestern University, Evanston, Illinois 60208, USA*
[15]*The Ohio State University, Columbus, Ohio 43210, USA*
[16]*University of Oklahoma, Norman, Oklahoma 73019, USA*
[17]*University of Pittsburgh, Pittsburgh, Pennsylvania 15260, USA*
[18]*Purdue University, West Lafayette, Indiana 47907, USA*
[19]*Rensselaer Polytechnic Institute, Troy, New York 12180, USA*
[20]*University of Rochester, Rochester, New York 14627, USA*
(Received 29 December 2003; published 11 June 2004)

We present the first study of the vector (Wess-Zumino) current in $\tau^- \to K^-\pi^-K^+\nu_\tau$ decay using data collected with the CLEO III detector at the Cornell Electron Storage Ring. We determine the quantitative contributions to the decay width from the vector and axial vector currents. Within the framework of a model by Kühn and Mirkes, we identify the quantitative contributions to the total decay rate from the intermediate states $\omega\pi$, $\rho^{(\prime)}\pi$, and K^*K.

DOI: 10.1103/PhysRevLett.92.232001 PACS numbers: 13.35.Dx, 11.40.–q

Hadronic τ decays provide a powerful tool to study low energy strong-interaction physics. The decay $\tau^- \to K^-\pi^-K^+\nu_\tau$ can proceed via both the vector and axial vector currents [1]; the vector current proceeds via the Wess-Zumino mechanism [2]. This model-independent mechanism plays an important role in hadron dynamics. It is applicable to τ decays [1,3] with three or more hadrons in the final state and violates the rule that the vector and axial vector currents produce an even and an odd number of pseudoscalars, respectively. Further interest in this decay is motivated by the fact that more precise knowledge of the $K\pi\bar{K}$ mass spectrum near the τ mass is essential to give more stringent constraints on the τ neutrino mass [4]. In this Letter, we present the first study of the vector (Wess-Zumino) current, as well as the axial vector current, in the decay $\tau^- \to K^-\pi^-K^+\nu_\tau$, and

determine their quantitative contributions to the decay width. Charge conjugate decays are implied throughout this Letter.

In the standard model, the general form for the Cabibbo-allowed semileptonic τ decay matrix element can be expressed as $\mathcal{M} = (G/\sqrt{2})V_{ud}\bar{u}(q_\nu)\gamma^\mu(1-\gamma_5)u(q_\tau)J^\mu$, where G is the Fermi coupling constant, V_{ud} is a Cabibbo-Kobayashi-Maskawa matrix element, q_ν and q_τ are the four-momenta of the τ neutrino and the τ lepton, respectively, $J^\mu \equiv \langle \text{hadrons}|V^\mu - A^\mu|0\rangle$ is the hadronic current, and V^μ and A^μ are, respectively, the vector and the axial vector quark currents. The most general ansatz for the hadronic current of three hadrons is characterized by four form factors [5] in terms of the hadrons' momenta q_i (here, $i = 1$ for K^-, $i = 2$ for π^-, and $i = 3$ for K^+),

$$J^\mu = \left(q_1^\mu - q_3^\mu - Q^\mu \frac{Q(q_1 - q_3)}{Q^2}\right)F_1(s_1, s_2, Q^2) + \left(q_2^\mu - q_3^\mu - Q^\mu \frac{Q(q_2 - q_3)}{Q^2}\right)F_2(s_1, s_2, Q^2) + i\epsilon^{\mu\alpha\beta\gamma}q_{1\alpha}q_{2\beta}q_{3\gamma}F_3(s_1, s_2, Q^2) + Q^\mu F_4(s_1, s_2, Q^2), \quad (1)$$

where $Q^\mu = q_1^\mu + q_2^\mu + q_3^\mu$. All four form factors F_1 through F_4 are functions of $Q^2 = (q_1 + q_2 + q_3)^2$, $s_1 = (q_2 + q_3)^2$, $s_2 = (q_1 + q_3)^2$, and $s_3 = (q_1 + q_2)^2$. The terms proportional to F_1 and F_2 originate from the axial vector current ($J^P = 1^+$). The vector current ($J^P = 1^-$) originating from the Wess-Zumino mechanism gives rise to the term proportional to F_3. F_4 is due to the spin-zero scalar current ($J^P = 0^+$) that is expected to be small [1,6] and in this analysis it will be set to zero, although we consider its contribution to the systematic uncertainties later.

Tau decay to three mesons is conveniently analyzed in the hadronic rest frame, where $\mathbf{q}_1 + \mathbf{q}_2 + \mathbf{q}_3 = \mathbf{0}$. The angle β [5] is defined as the angle between the direction of the hadronic system in the laboratory frame and the normal to the plane defined by the momenta of particles 1 and 2,

$$\cos\beta = -\hat{\mathbf{Q}} \cdot \text{norm}(\hat{\mathbf{q}}_1 \times \hat{\mathbf{q}}_2). \quad (2)$$

The angle θ [5], defined to be the angle between the flight direction of the τ lepton in the laboratory frame and the direction of the hadronic system as seen in the τ rest frame, is related to the energy E_h of the hadronic system in the laboratory frame by

$$\cos\theta = \frac{2xm_\tau^2 - m_\tau^2 - Q^2}{(m_\tau^2 - Q^2)\sqrt{1 - 4m_\tau^2/s}}, \quad (3)$$

where $x = 2E_h/\sqrt{s}$ and s is the square of the center of mass energy. The angle ψ [5] between the flight direction of the τ lepton and that of the laboratory frame as seen from the hadronic rest frame, $-\hat{\mathbf{Q}}$, is given by

$$\cos\psi = \frac{x(m_\tau^2 + Q^2) - 2Q^2}{(m_\tau^2 - Q^2)\sqrt{x^2 - 4Q^2/s}}. \quad (4)$$

The differential decay width for the decay $\tau^- \to K^-\pi^-K^+\nu_\tau$ with the scalar contribution neglected, after integrating over the unobserved neutrino direction, is given [5] by

$$\frac{d\Gamma(\tau \to K\pi\bar{K}\nu_\tau)}{dQ^2 ds_1 ds_2} = \frac{G^2}{12m_\tau}|V_{ud}|^2 \frac{1}{(4\pi)^5}\frac{(m_\tau^2 - Q^2)^2}{Q^4} \times \left\{\left(1 + \frac{2Q^2}{m_\tau^2}\right)(W_A + W_B)\right\}. \quad (5)$$

Here, the structure functions W_A and W_B can be expressed in terms of the form factors as

$$W_A = (x_1^2 + x_3^2)|F_1|^2 + (x_2^2 + x_3^2)|F_2|^2 + 2(x_1x_2 - x_3^2)\text{Re}(F_1F_2^*), \quad W_B = x_4^2|F_3|^2, \quad (6)$$

where x_i [5] are known functions of Q^2, s_1, s_2, and s_3. Thus W_A and W_B govern the rate and the distributions of Q^2, s_1, s_2, and s_3. There is no interference between the axial vector current contributions (F_1, F_2) and the vector current contribution (F_3) to the decay width.

A parametrization of the form factors is given in [6], based on chiral perturbation theory at low momenta and meson resonance dominance at higher momenta. It has been implemented in the Monte Carlo program KORALB [7] as

$$F_1 = -\frac{\sqrt{2}}{3f_\pi}\text{BW}_{a_1}(Q^2)\frac{\text{BW}_\rho(s_2) + \beta_\rho \text{BW}_{\rho'}(s_2)}{1 + \beta_\rho},$$
$$F_2 = -\frac{\sqrt{2}}{3f_\pi}R_F\text{BW}_{a_1}(Q^2)\text{BW}_{K^*}(s_1),$$
$$F_3 = -\frac{1}{2\sqrt{2}\pi^2 f_\pi^3}\sqrt{R_B}\frac{\text{BW}_\omega(s_2) + \alpha\text{BW}_{K^*}(s_1)}{1 + \alpha} \times \frac{\text{BW}_\rho(Q^2) + \lambda\text{BW}_{\rho'}(Q^2) + \delta\text{BW}_{\rho''}(Q^2)}{1 + \lambda + \delta}, \quad (7)$$

where $f_\pi = 0.0933$ GeV and $\beta_\rho = -0.145$ [6,7]. $\text{BW}_X(s)$ is the two- (dependent on s_1 or s_2) or three- (dependent on Q^2) particle Breit-Wigner propagator with an energy dependent width. The CLEO result on the a_1 parametrization derived from $\tau^- \to \pi^-\pi^0\pi^0\nu_\tau$ decay [8] is used. The parametrizations of two-particle Breit-Wigner functions take the forms used in [6]. The parameters used for the three-particle Breit-Wigner functions are taken from the

Particle Data Tables [9]: $m_\rho = 0.770$ GeV, $\Gamma_\rho = 0.151$ GeV, $m_{\rho'} = 1.465$ GeV, $\Gamma_{\rho'} = 0.310$ GeV, $m_{\rho''} = 1.700$ GeV, and $\Gamma_{\rho''} = 0.240$ GeV.

The form factors F_1 and F_2 correspond to the axial vector current processes $a_1 \to \rho^{(\prime)}\pi^-$ with $\rho^{(\prime)} \to K^-K^+$ and $a_1 \to K^*K^-$ with $K^* \to K^+\pi^-$, respectively. The form factor F_3 represents the vector current processes $\rho^{(\prime,\prime\prime)}$ decays to K^*K^- and $\omega\pi^-$ with $K^* \to K^+\pi^-$ and $\omega \to K^-K^+$. G parity conservation forbids the vector current process $W^- \to \rho^{(\prime,\prime\prime)} \to \rho^{(\prime)}\pi^-$ with $\rho^{(\prime)} \to K^-K^+$. Instead, in [6] the process $W^- \to \rho^{(\prime,\prime\prime)} \to \omega\pi^-$ is considered, although the subsequent decay $\omega \to K^-K^+$ proceeds only through the high-mass tail of its Breit-Wigner propagator. We make use of this model in this analysis, although we are unable to distinguish whether the decay proceeds via the ω meson or via some other resonance with pole mass outside the kinematic limits for the $K\bar{K}$ mass.

The default version of KORALB [7] does not model the decay $\tau^- \to K^-\pi^-K^+\nu_\tau$ well, as indicated by the discrepancies in describing the invariant mass distributions [10]. To improve the agreement, we introduce two more parameters R_B and R_F, describing the relative strengths of W_B and W_A and of F_2 and F_1 in Eqs. (5) and (6). These two parameters are explicitly expressed in our generalization of the form factors in Eq. (7). The five model parameters α, λ, δ, R_B, and R_F are determined in this analysis by a simultaneous fit to the invariant mass spectra of $K^-\pi^-K^+$, $K^+\pi^-$, and K^-K^+. These five parameters allow for a fit that properly describes all the mass spectra. In general, these parameters should be complex, allowing additional interferences. However, due to limited statistics, we have set them real and taken into account only the inherent phase of the Breit-Wigner functions in Eq. (7).

The data sample used for this analysis corresponds to an integrated luminosity of 7.77 fb^{-1} taken on or near the $\Upsilon(4S)$. It contains about 7.09×10^6 tau pairs. The data were collected with the CLEO III detector [11] located at the e^+e^- Cornell Electron Storage Ring. The CLEO III detector configuration features a four-layer silicon strip vertex detector, a wire drift chamber, and, most importantly for this analysis, a ring imaging Cherenkov (RICH) particle identification system. A detailed description of the RICH performance can be found in [12].

To select the three-prong τ decays to the $K^-\pi^-K^+\nu_\tau$ final state, we use one-prong decays of the other τ to $e^+\nu\nu$, $\mu^+\nu\nu$, $\rho^+\nu$, and $\pi^+(K^+)\nu$ to tag tau-pair events. Pion and kaon identification is obtained by a combination of the RICH information with dE/dx measured in the drift chamber. We use the event selection criteria listed in [13] and find 2255 candidate signal events in our data sample. The branching fraction obtained using this data sample for the decay $\tau^- \to K^-\pi^-K^+\nu_\tau$ is consistent with the previously published result [13].

Background contributions and efficiencies are obtained using Monte Carlo events from the KORALB [7] and JETSET [14] generators for the tau-pair production and $q\bar{q} \to$ hadron processes, respectively. These events are then processed by the GEANT-based [15] CLEO detector simulation and pattern reconstruction. In our sample, $256 \pm 16 \pm 46$ events are attributed to the backgrounds from the continuum $q\bar{q}$ production and from tau decays to other channels. The dominant backgrounds are due to pion misidentification or missing π^0 from the tau cross-feed decays $\tau^- \to K^-\pi^+\pi^-\nu_\tau$, $\pi^-\pi^+\pi^-\nu_\tau$, and $K^-\pi^-K^+\pi^0\nu_\tau$, or from $\tau^- \to K^-\pi^-K^+\nu_\tau$ decay with a misidentified tag side. Each of these sources contributes about 20% of the total backgrounds. The events with the three-prong side identified as $K^-\pi^-K^+\nu_\tau$ and the tag side misidentified are analyzed in the same way as the signals.

We use the unbinned extended maximum likelihood method to extract the parameters of the hadronic structure of the decay described above. The likelihood function, $\mathcal{L}$, has the form

$$\mathcal{L} = \frac{e^{-m}m^n}{n!}\prod_{i=1}^{n}\frac{1}{n}\{N^S\mathcal{P}_i^S(\alpha, \lambda, \delta, R_B, R_F, Q^2, s_1, s_2) + N^B\mathcal{P}_i^B(\alpha, \lambda, \delta, R_B, R_F, Q^2, s_1, s_2)\}. \quad (8)$$

The numbers of signal and background events are denoted by N^S and N^B with $n = N^S + N^B$. m is the number of the expected events. $\mathcal{P}_i^S$ and $\mathcal{P}_i^B$ represent the normalized probability density functions (PDFs) for event i to be either a signal or a background event. The signal PDF is formed from the product of one-dimensional PDFs obtained from integrations over the differential decay width described by Eq. (5), convoluted with the mass-dependent efficiencies. The background PDFs are obtained from Monte Carlo simulations. The fitting procedure has been tested with Monte Carlo samples to verify its performance.

The results of the unbinned extended maximum likelihood fits are projected onto the $K^-\pi^-K^+$, $K^+\pi^-$, and K^-K^+ mass axes with different contributions superimposed as illustrated in Fig. 1. We observe that about half of the τ decay to $K^-\pi^-K^+\nu_\tau$ proceeds via the vector (Wess-Zumino) current. The fit parameters are $\alpha = 0.471 \pm 0.060$, $\lambda = -0.314 \pm 0.073$, $\delta = 0.101 \pm 0.020$, $R_B = 3.23 \pm 0.26$, and $R_F = 0.98 \pm 0.15$ (statistical errors only). The angular distributions of $\cos\beta$, $\cos\theta$, and $\cos\psi$ for the data and for the two Monte Carlo samples generated using the parameters from the fits are shown in Fig. 2. The comparison shows that the Monte Carlo samples with and without the contribution from the vector (Wess-Zumino) current both describe the data well within the current statistics; the angular observables therefore have little sensitivity to the presence of the vector (Wess-Zumino) current in our sample. Our ability to distinguish the axial vector contribution from the

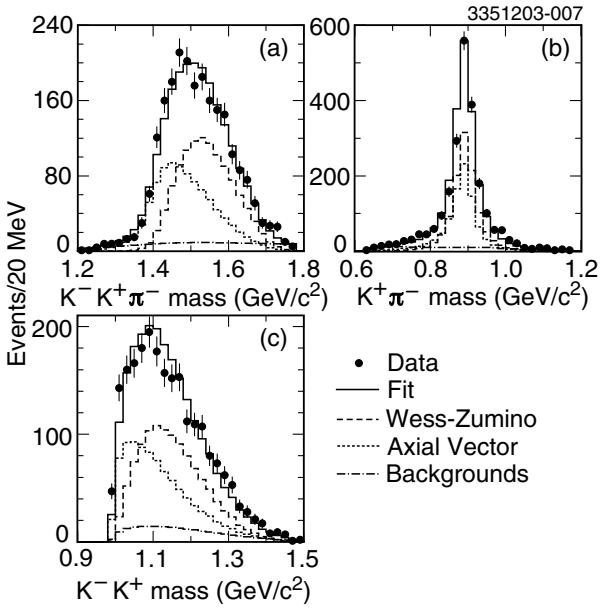

FIG. 1. Projections of the fits (full lines) onto the (a) $K^-\pi^-K^+$, (b) $K^+\pi^-$, and (c) K^-K^+ mass axes from the data (dots with error bars) superimposed with the contributions from the vector (Wess-Zumino) current (dashed line) and the axial vector current (dotted line) and all backgrounds (dot-dashed line).

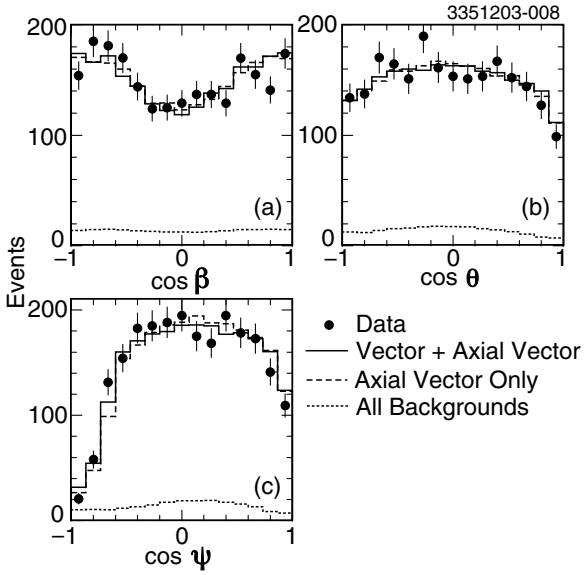

FIG. 2. Angular distributions of (a) $\cos\beta$, (b) $\cos\theta$, and (c) $\cos\psi$ for the data with statistical errors only. The solid lines represent our model of the vector (Wess-Zumino) and axial-vector signal contributions and all backgrounds, using the parameters from the full fit to the data. The dashed lines represent our model of signal and backgrounds with the vector (Wess-Zumino) contribution excluded. The dotted lines show all backgrounds.

vector (Wess-Zumino) contribution comes from the invariant mass distributions and thus depends on the correct modeling of the associated form factors, as constrained by our data.

We have considered the following sources of systematic errors: the systematic errors for the five model parameters and for the fractions of the vector and axial vector current contributions to the decay rate (including those of the intermediate states) come from the mass dependence of the detection efficiency, from the uncertainties in the modeling of the mass resolutions, from the uncertainties in the parametrizations of the resonances, and from the neglected contribution of the scalar current. To estimate the effects of the detection efficiencies, we introduce an artificial linear mass dependence of the efficiencies and vary the corresponding slopes by $\pm 10\%$. We estimate the associated systematic error on the relative strength of the vector and axial vector currents as $\Delta R_B/R_B = 10\%$. The corresponding systematic errors on all other fit parameters and the fractions of the vector and axial vector current contributions to the decay rate are less than 4% of their values. The typical mass resolutions of the hadronic final state in the decay $\tau^- \to K^-\pi^-K^+\nu_\tau$ are about 2–3 MeV, i.e., much smaller than the widths of the resonances considered. The uncertainty in the modeling of the detector resolutions contributes a $<2\%$ systematic error. The uncertainty introduced by the neglected scalar current is estimated at the model predicted level [6,7] and found to be less than 1%. In addition, when we vary the normalization and the shapes of the background PDFs by $\pm 1\sigma$, the fit results vary between 1% and 12%. When the parameter β_ρ in Eq. (7) varied by $\pm 100\%$, the results change 37% for the parameter R_F and less than 3% for all other fit parameters and the contributions of the vector and axial vector currents. The dominant uncertainty in the fit results arises from the errors of the parametrizations of the poorly measured ρ' and ρ'' resonances [9]. The corresponding contribution to the overall systematic uncertainties for the parameters α, λ, δ, R_B, and R_F is 5%, 23%, 153%, 56%, and 1%, respectively. Similarly, it is 8%, 10%, 11%, 12%, 9%, and 27% for the fractions $\mathcal{R}_{\rm WZ}$, $\mathcal{R}_{\rm AV}$, $\mathcal{R}_{\rm AV}^{K^*K}$, $\mathcal{R}_{\rm AV}^{\rho^{(\prime)}\pi}$, $\mathcal{R}_{\rm WZ}^{K^*K}$, and $\mathcal{R}_{\rm WZ}^{\omega\pi}$ to be presented. We add all estimates of the systematic errors in quadrature and obtain the overall systematic uncertainties for the five parameters α (7%), λ (25%), δ (154%), R_B (59%), and R_F (37%) and for the fractions $\mathcal{R}_{\rm WZ}$ (9%), $\mathcal{R}_{\rm AV}$ (11%), $\mathcal{R}_{\rm AV}^{K^*K}$ (11%), $\mathcal{R}_{\rm AV}^{\rho^{(\prime)}\pi}$ (16%), $\mathcal{R}_{\rm WZ}^{K^*K}$ (10%), and $\mathcal{R}_{\rm WZ}^{\omega\pi}$ (29%). There is a large uncertainty in the contribution of the ρ'' resonance to the vector current. This has little effect on the total vector contribution because it is strongly suppressed by phase space, and its contribution is easily absorbed into the contribution from the ρ' resonance.

In summary, we have presented the first study of the vector (Wess-Zumino) current in the decay $\tau^- \to K^-\pi^-K^+\nu_\tau$ and determined its contribution, as well as that from the axial vector current, to be

$$\mathcal{R}_{\mathrm{WZ}} = \frac{\Gamma_{\mathrm{WZ}}}{\Gamma_{\mathrm{tot}}} = (55.7 \pm 8.4 \pm 4.9)\%,$$
$$\mathcal{R}_{\mathrm{AV}} = \frac{\Gamma_{\mathrm{AV}}}{\Gamma_{\mathrm{tot}}} = (44.3 \pm 8.4 \pm 4.9)\%. \quad (9)$$

The errors are statistical and systematic, respectively.

The structure of the decay $\tau^- \to K^-\pi^-K^+\nu_\tau$ can be modeled using the parametrization given by Eqs. (5)–(7), with the parameters determined to be $\alpha = 0.471 \pm 0.060 \pm 0.034$, $\lambda = -0.314 \pm 0.073 \pm 0.080$, $\delta = 0.101 \pm 0.020 \pm 0.156$, $R_B = 3.23 \pm 0.26 \pm 1.90$, and $R_F = 0.98 \pm 0.15 \pm 0.36$.

In the context of the model by Kühn and Mirkes [5], where the axial vector current proceeds via $a_1 \to \rho^{(\prime)}\pi^-$ and $a_1 \to K^*K^-$, and the vector (Wess-Zumino) current via $\rho^{(\prime,\prime\prime)} \to K^*K^-$ and $\omega\pi^-$, we can also separate the individual contributions from the intermediate states $\omega\pi^-$, $\rho^{(\prime)}\pi^-$, and K^*K^- to the total decay width as

$$\mathcal{R}_{\mathrm{WZ}}^{\omega\pi} = \frac{\Gamma_{\mathrm{WZ}}^{\omega\pi}}{\Gamma_{\mathrm{tot}}} = (3.4 \pm 0.9 \pm 1.0)\%,$$
$$\mathcal{R}_{\mathrm{AV}}^{\rho^{(\prime)}\pi} = \frac{\Gamma_{\mathrm{AV}}^{\rho^{(\prime)}\pi}}{\Gamma_{\mathrm{tot}}} = (2.5 \pm 0.8 \pm 0.4)\%,$$
$$\mathcal{R}_{\mathrm{WZ}}^{K^*K} = \frac{\Gamma_{\mathrm{WZ}}^{K^*K}}{\Gamma_{\mathrm{tot}}} = (60.8 \pm 8.5 \pm 6.0)\%, \quad (10)$$
$$\mathcal{R}_{\mathrm{AV}}^{K^*K} = \frac{\Gamma_{\mathrm{AV}}^{K^*K}}{\Gamma_{\mathrm{tot}}} = (46.8 \pm 8.4 \pm 5.2)\%.$$

These fractions do not add up to 100% due to the interference of the amplitudes of the intermediate states. The decay is dominated by the vector (Wess-Zumino) and axial vector current processes via the intermediate state K^*K. The ratio $R_{\mathrm{AV}}^{K^*K}$, together with $\mathcal{B}(\tau^- \to K^-\pi^-K^+\nu_\tau)$ [13], yields $\mathcal{B}(a_1 \to K^*K) = (2.2 \pm 0.5)\%$ which is compatible with the result $\mathcal{B}(a_1 \to K^*K) = (3.3 \pm 0.5)\%$ extracted from the decay $\tau^- \to \pi^-\pi^0\pi^0\nu_\tau$ [8] with only one threshold (K^*K) considered. The apparent shortfall of the $\pi^-\pi^0\pi^0$ mass spectrum in the previous analysis is attributed to the neglected contribution from the vector (Wess-Zumino) current. The axial vector current contribution determined in this Letter is much lower than the result from ALEPH [16] based on the conserved vector current hypothesis and limited e^+e^- data. As noted above, we cannot distinguish the $\rho^{(\prime,\prime\prime)} \to \omega\pi^-$ with $\omega \to K^-K^+$ decay from other models, such as other vector meson resonances or even a simple constant. Setting the $\omega\pi^-$ contribution to zero, we obtain $\mathcal{R}_{\mathrm{WZ}}^{(K^*K)} = (50.8 \pm 7.7)\%$, $\mathcal{R}_{\mathrm{AV}} = (49.2 \pm 7.7)\%$, $\mathcal{R}_{\mathrm{AV}}^{\rho^{(\prime)}\pi} = (4.5 \pm 1.4)\%$, and $\mathcal{R}_{\mathrm{AV}}^{K^*K} = (51.6 \pm 7.8)\%$. However, the fit favors the presence of an additional resonance component, which can be associated, within the context of the model in [6], with $\omega\pi^-$, over its absence by nearly 6σ (statistical error only). The model parameters presented here can reduce the model dependent uncertainties on the tau neutrino (ν_τ) mass measurements using the decay $\tau^- \to K^-\pi^-K^+\nu_\tau$.

We gratefully acknowledge the effort of the CESR staff in providing us with excellent luminosity and running conditions. This work was supported by the National Science Foundation, by the U.S. Department of Energy, by the Research Corporation, and by the Texas Advanced Research Program.

[1] R. Decker *et al.*, Phys. Rev. D **47**, 4012 (1993).
[2] J. Wess and B. Zumino, Phys. Lett. **37B**, 95 (1971).
[3] B. A. Li, Phys. Rev. D **55**, 1425 (1997); **55**, 1436 (1997); **57**, 1790 (1998).
[4] DELCO Collaboration, G. B. Mills *et al.*, Phys. Rev. Lett. **54**, 624 (1985); D. L. Perego, Nucl. Phys. B (Proc. Suppl.) **123**, 251 (2003).
[5] J. H. Kühn and E. Mirkes, Z. Phys. C **56**, 661 (1992).
[6] R. Decker *et al.*, Z. Phys. C **58**, 445 (1993); M. Finkemeier and E. Mirkes, Z. Phys. C **69**, 243 (1996).
[7] S. Jadach and Z. Was, Comput. Phys. Commun. **36**, 191 (1985); **64**, 267 (1991); **76**, 361 (1993); **85**, 453 (1995).
[8] All CLEO results on the branching fractions and resonance contents of the decays $\tau^- \to (3\pi)^-\nu_\tau$ have been implemented in the CLEO version of the KORALB Monte Carlo program [7]. For experimental results, see D. M. Asner *et al.*, Phys. Rev. D **61**, 012002 (2000); see also A. Weinstein, Nucl. Phys. B (Proc. Suppl.) **123**, 107 (2003).
[9] Particle Data Group, K. Hagiwara *et al.*, Phys. Rev. D **66**, 010001 (2002).
[10] F. Liu, Nucl. Phys. B (Proc. Suppl.) **123**, 66 (2003).
[11] CLEO Collaboration, Y. Kubota *et al.*, Nucl. Instrum. Methods Phys. Res., Sect. A **320**, 66 (1992); T. Hill, Nucl. Instrum. Methods Phys. Res., Sect. A **418**, 32 (1998); D. Peterson *et al.*, Nucl. Instrum. Methods Phys. Res., Sect. A **478**, 142 (2002); T. Coan, Nucl. Instrum. Methods Phys. Res., Sect. A **379**, 448 (1996).
[12] M. Artuso *et al.*, Nucl. Instrum. Methods Phys. Res., Sect. A **502**, 91 (2003).
[13] CLEO Collaboration, R. Briere *et al.*, Phys. Rev. Lett. **90**, 181802 (2003).
[14] T. Sjostrand, CERN Report No. CERN-TH-6488-92 (unpublished).
[15] R. Brun *et al.*, GEANT3.14, CERN Report No. CERN DD/EE/84-1 (unpublished).
[16] ALEPH Collaboration, R. Barate *et al.*, Eur. Phys. J. C **11**, 599 (1999).